[redacted]

N65-88731

38 p

[redacted]

DIRECTIONAL FLUX DENSITIES AND MIRROR-POINT DISTRIBUTIONS OF TRAPPED PARTICLES FROM SATELLITE 1958 EPSILON MEASUREMENTS[1]

C. A. Lundquist, R. J. Naumann, and
A. H. Weber[2]

George C. Marshall Space Flight Center
Aeronautics and Space Administration
Huntsville, Alabama

May 1, 1962

FACILITY FORM 602

N65-88731 (ACCESSION NUMBER) | (THRU)

38 (PAGES) | (CODE)

TMX-57445 (NASA CR OR TMX OR AD NUMBER) | (CATEGORY)

[1] submitted for publication in the Journal of Geophysical Research

[2] also Physics Department, Saint Louis University

ABSTRACT

14971

Satellite 1958 Epsilon (Explorer IV) contained a directional plastic scintillation counter, prepared by Van Allen and associates, mounted with its axis perpendicular to the long symmetry axis of the satellite. Count-rate data from this detector have been analyzed to yield directional flux densities (particles/cm^2-sec-sr) of geomagnetically trapped charged particles as a function of the angle with the perpendicular to the magnetic field. The analysis employs a new determination by E. O. Baicy of the directional response of the detector and detailed geomagnetic field information supplied through the courtesy of J. A. Welch, Jr. of the Air Force Special Weapons Center. The direction of the counter axis as a function of time is determined from the modulations of ground-received r-f signal strengths and detector counting rates produced by the body motions of the satellite. The directional particle flux densities are calculated by computer solutions of the integral equation relating observed count rates and the particle flux densities. Mirror point distributions of the charged particles along magnetic field lines extending from the satellite position to lower altitudes are obtained directly from the particle flux density calculations. The data are presented both in terms of geographic coordinates and the dynamical invariants.

Available to NASA Offices and NASA Centers Only.

1. INTRODUCTION

The content of the Van Allen belts of charged particles trapped by the geomagnetic field has been investigated quite extensively, both theoretically and experimentally. The broad features of the radiation belts now seem to be fairly definite. These features are indicated by the sketch in Fig. 1 and the tabulated information contained in Table 1. They may be summarized by the following:

(1) Charged particles, both positive and negative, of greater than thermal energies are present from roughly 10^3 to 40×10^3 km in altitude. The apparent absence of any extensive and significant electric fields precludes any large-scale positive - negative charge separation.

(2) The proton content of the belts may be described partially by these items:

(a) The interesting component of the proton content is the energetic (10 - 1000 mev, approximately) flux which peaks at about 3.7×10^3 km in altitude (Fig. 1) within the inner belt.

(b) This hard proton component can be accounted for in part by the neutron albedo mechanism. The flux-energy spectrum is that expected from the fast neutron decays except for a deficiency of protons at the higher energies.

(c) The stated deficiency of energetic protons can be explained by these several mechanisms (separately,

or in combination): breakdown of magnetic moment invariance [Singer, 1959] ; trapped solar protons [Naugle and Kniffen, 1961] (which produce an excess of lower energy protons); protons produced at lower energies by albedo neutrons in turn resulting from solar protons interacting with atmospheric nuclei in the polar regions [Naugle and Kniffen, 1961]; loss of geomagnetically trapped protons by nuclear collisions [Freden and White, 1960] .

(d) Both the flux and the flux-energy spectrum of the hard proton component change with latitude [Naugle and Kniffen, 1961].

(e) Hydromagnetic scattering [Welch and Whitaker, 1959; Dragt, 1961] and/or failure of invariance of proton magnetic moment [Singer, 1959; Lenchek and Singer, 1960] limit energetic protons to lower altitudes and so account for their absence in the outer belt.

(3) The electrons of the belts are characterized partially, as follows:

(a) The electron flux exhibits at least two maxima (Fig. 1), the inner belt maximum located quite definitely at about 9.6×10^3 km altitude, and the outer belt located not so definitely near 18×10^3 km altitude. About halfway between the two belts, near

12.8×10^3 km altitude is the minimum in electron flux of the "slot."

(b) The geomagnetically trapped electrons which have been detected by the various satellites, rockets, and space probes in both belts are in the general range 30 kev - 1 mev. The electron flux in this energy range is about 100 times the flux of both electrons and protons of energies greater than 1 mev.

(c) The electrons in the experimentally observed range up to about 1 mev in both belts apparently can be accounted for, again in part, by the neutron albedo source mechanism. The flux-energy spectrum is that expected from a slow neutron decay with energy degradation, presumably by electron-electron collisions, yielding a spectrum somewhat softer than the 750-kev end-point energy β-decay spectrum of slow neutrons [Holly et al, 1961; Walt et al, 1960; Dessler and Karplus, 1960; Vernov et al, 1959].

(d) A simple explanation for the electron flux minimum between the two belts has been suggested by Dessler and Karplus [1960]. Their analysis employs the lowering of electron mirror points in the region of the Capetown anomaly along with the corresponding atmospheric absorption of the particles to account for the absence of trapped particles at altitudes corresponding to the "slot" of Fig. 1. Quite to the

contrary, [R. A. Hoffman, 1961] concludes from Explorer VI data that charged particles which are affected by the Capetown anomaly do not pass through the observed minimum between the inner and outer belts. This conclusion is based on the accuracy of the present magnetic data, but rather considerable magnetic field errors are required to invalidate the conclusion.

Herlofson [1960] has shown that different diffusion times for electrons injected at the outer edge of the outer belt could account for the two electron belts and the slot between them — an entirely different mechanism.

(e) The observed large fluctuations of the outer belt electron flux may be, in part, apparent rather than real; that is, changes in count rate may be due to electron energy changes. Such electron energy changes can cause large numbers of electrons to shift either below or above energy thresholds of detectors causing decreases or increases in count rates.

It seems clear that energy change mechanisms account for at least part of the observed electron flux variations [Van Allen, 1959; Dessler and Karplus, 1960; Arnoldy et al, 1960; Helliwell and Bell, 1960]. Recently, Dessler and Karplus [1961] have considered quantitatively the effect of distortions of the geomagnetic field caused by diamagnetic ring currents such as the magnetic storm main phase ring

current. A sequence of events in the outer belt may be summarized as follows:

(1) Electrons are deposited throughout the entire geomagnetic field with a trapping time of the order of 10^9 sec and the low energy trapped radiation distends the geomagnetic field at distances of 6 - 11 earth radii.

(2) A diamagnetic ring current is produced at 3 - 5 earth radii by a geomagnetic storm and this current results in a deceleration of the trapped particles and a consequent decrease in counting rates of observing instruments.

(3) The distortions in the geomagnetic field due to the storm result in a loss of the low energy particles trapped at 6 - 11 earth radii so that, following the decay of the magnetic storm ring current, the magnetic field contracts beyond its prestorm configuration producing through adiabatic compression an increase in energy, along with increased count rates, of electrons which are present. This kind of reversible betatron mechanism can explain part but not all of the observed effects as has been shown by Rosen and Farley [1961] in their consideration of Explorer VI radiation count rates — a conclusion agreed to by Dessler and Karplus [1961].
It should be emphasized, as pointed out by R. Kaufmann and S. F. Singer [1961] (discussions at a meeting of the American Geophysical Union, University of California at Los Angeles, December 1961) that there are available a variety of mechanisms suitable for particle acceleration;

what is needed is experimental evidence to aid in evaluating these several mechanisms.

(4) The effect of charged particle injection from the sun is not clear (see Table 1). Freden and White [1960] found no evidence for solar protons in the inner belt but Naugle and Kniffen [1961] imply that the question is still open. Dessler and Karplus [1960] consider solar electron injection into the inner belt inconsistent with observations. Cladis and Dessler [1961] and Arnoldy et al [1960] come to the same conclusion regarding the outer belt.

(5) Finally, it appears that the neutron albedo mechanism contributes significantly to the number of geomagnetically trapped electrons and protons at all distances out to 7 earth radii or more from the earth's center. Various other effects including solar injection and energy change mechanisms are also possible and operative.

Recent evidence indicates that the neutron albedo mechanism cannot be the sole source of trapped protons and electrons. Kellogg [1960] originally raised serious questions about the mechanism. Also quite recently, E. C. Ray and Carl McIlwain (discussions at meeting of AGU, UCLA, 1961; op. cit.) have raised fresh doubts relative to the neutron albedo hypothesis because of the large numbers of electrons and protons which have been detected in the inner belt. The electron fluxes appear to be excessive by 2 to 3 orders of magnitude and the proton fluxes by 4 to 5 orders. Their evidence is based upon flux

magnitudes without very definite energy discrimination.

Lenchek, Singer and Wentworth [1961] have compared the neutron albedo theory for trapped electrons with experimental observations. They calculate the differential omnidirectional electron flux density (electrons/cm^2-sec-kev) vs. energy due to a neutron albedo source coupled with energy loss by Coulomb interactions (involving small angle scattering only) in the residual atmosphere (average effective density of scattering centers, $9.7 \times 10^4/cm^3$) at 1100 km altitude on a magnetic B line extending to 1.5 earth radii. For experimental comparison they use the observations of Walt, Chase, Cladis, Imhof and Knecht [1960, 1961] and Holly [1960] and conclude that the albedo theory and their energy loss mechanism agree quantitatively for electron energies above about 400 kev. Hess, Killeen et al [1961] compare calculations and experiments to conclude that neutron decay electrons contribute significantly to the electron fluxes of the outer belt.

In the present report, analyses of the count-rate vs. time of the directional detector (Detector A) carried by satellite 1958 Epsilon (Explorer IV) are employed to calculate both the directional particle flux density and the corresponding mirror point distribution of the geomagnetically trapped particles, thus yielding further detailed information about this phenomenon.

2. EXPERIMENTAL ASPECTS

The radiation detection instrumentation used in earth satellite 1958 Epsilon (Explorer IV) has been described in detail by Van Allen [1959] and his group. The present investigation, involving further analysis of the extensive data obtained and interpreted by Van Allen, was motivated by the possibility of determining directional radiation intensities [Lundquist et al, 1962]. Of interest for the directional counting analysis is Detector A (a plastic scintillator, 0.75 cm in diameter and 0.18 cm thick, mounted on a photomultiplier tube) having its scintillator located adjacent to a circular hole in the cylindrical shell of the satellite so that the detector axis is perpendicular to the long axis of the satellite. Radiation passing through the hole penetrated a 140-mg/cm^2 Al absorber to reach the scintillator, where an additional electronic bias produced these radiation thresholds [Baicy et al, 1962]: 700 kev for electrons, 10 mev for protons, and 300 kev for X-rays. Other radiation detected had to penetrate the steel wall of the satellite and any other intervening material. The geometry of the aperture and detector were such as to produce a detector response $S(\alpha)$ vs. angle α of incoming radiation with detector-axis, as indicated by Fig. 2b. Thus, the radiation passing through the hole in the satellite shell and penetrating 140 mg/cm^2 of Al, was counted only when entering the hole at a relatively small angle with the counter axis. The Explorer IV detectors, calibrated originally by Van Allen, were recalibrated in greater detail by E. O. Baicy and associates [1962] employing a duplicate payload to investigate more fully the direction-dependent factors and the response to electrons.

The direction of the counter axis relative to a perpendicular to the geomagnetic flux density direction $\vec{B}$, represented by angle θ of Fig. 2b, has been determined as a function of time [Lundquist et al, 1962]. The satellite position (altitude, latitude and longitude) and corresponding geomagnetic flux density magnitude B are known also as a function of time from the satellite ephemeris [Adams, 1959; Jensen, et al, 1960]. These two groups of information plus the Detector A count rate as a function of time are used in the present work to determine the directional radiation flux density in space. Further information about charged particle trapping in the geomagnetic field is then derived.

The analyses involved are limited to situations in which the telemetry switching period is small compared to the mechanical roll and tumble periods of the satellite. Telemetry channel 5 switched frequency for each 16 and channel 2 for each 2048 accumulated scintillator counts. Further, an extended period of telemetry reception free from noise and signal fadeout is required. Only a small fraction of the total telemetry data received from Explorer IV satisfy these conditions on count rate and telemetry quality. However, a number of satisfactory telemetry records for satellite passes within range of the U. S. Army Tracking Station at Huntsville, Alabama do exist and of these a representative number (see Fig. 3) have been analyzed in the manner indicated above.

The cases so far analyzed correspond to satellite passes through parts of the inner Van Allen belt, the composition of which is believed to be quite time independent [Van Allen, 1959]. Limited evidence relating to the radiation constancy of the inner belt is included in the

present investigation, since data from corresponding satellite passes in the same region of space but at a time interval of about two days were analyzed. Suitable telemetry data for satellite passes through the artificial Argus belt [Van Allen, 1959] also exist and can be similarly analyzed.

From the results cited in Section 1 there is evidence, theoretical and experimental, that the observed Detector A count rates are due to electrons in a fairly narrow energy band. Holly, Allen and Johnson have used the study of Freden and White [1960] of the inner Van Allen belt protons to conclude that their own detector, a G-M counter with 150 mg/cm^2 (electron cutoff of about 460 kev) absorber, counts approximately 90% electrons and 10% protons [Holly et al, 1961; Fig. 4] at 980 km altitude and 15°N latitude. Detector A of Explorer IV had a 140-mg/cm^2 Al absorber over the window of the counter plus an additional electronic bias which excluded electrons of energy less than about 700 kev, and so should respond much like Holly's detector in the electron-proton field of the inner belt. Further, the assumption that the electron spectrum at altitudes near 1000 km and latitudes near 15°N (see Fig. 4 for spatial location of Explorer IV) is a degraded neutron β-decay spectrum (Table 1) yields the interesting conclusion that Detector A counts predominately electrons within fairly narrow limits centered near 700 kev.

3. DETERMINATION OF DIRECTIONAL PARTICLE FLUX DENSITY

From the analysis of the observed modulation of the transmitted r-f signal strength and counting rate produced by the roll and tumble of the Explorer IV satellite, Lundquist, Naumann, and Fields, [1962] were able to plot the true directional count rate of Detector A as a function of the angle θ between the counter detector axis and a perpendicular to the known [Jensen et al, 1960; Vestine and Sibley, 1960] magnetic flux density vector B . The geomagnetically trapped charged particle flux was observed to produce (Fig. 2c): (1) a count rate constant with θ , for θ greater than approximately 50°, and (2) a count rate $C_{obs}(\theta)$ dependent on θ , with the maximum corresponding to and symmetrical about $\theta = 0°$. The former was interpreted as due to hard components of the trapped particle radiation which were energetic enough, either directly or indirectly through their bremsstrahlung secondaries, to penetrate shielding material between the detector and outside space over the entire 4π solid angle about the detector. This count rate, apparently constant with θ , was subtracted from $C_{obs}(\theta)$ at all θ's to obtain the directional count rate. The latter was corrected for detector deadtimes [Van Allen, 1959; Baicy, 1962] and the result is designated $C'(\theta)$.

The detailed analysis of the characteristics of geomagnetically trapped charged particle radiation requires a determination of the directional particle flux density $J(\theta')$. The true directional count rate per unit area $C(\theta)$ (counts/cm²-sec) is related to $J(\theta')$ (particles/cm²-sec²-sr) by

$$C(\theta) = \frac{C'(\theta)}{A} = \int_{\text{all directions}} J(\theta')\, S(\alpha)\, d\Omega \quad \frac{\text{counts}}{\text{cm}^2\text{ - sec}} , \qquad (1)$$

where A is the area-efficiency factor (the product of the effective area and efficiency of the detector); $S(\alpha)$ is the response of the detector as a function of angle α ; and $J(\theta')$ is the required directional particle flux density for which the equation must be solved. For use in Eq. (1), $S(\alpha)$ is measured by calibration procedures [Baicy, 1962], and has the shape of Fig. 2b for 700-kev electrons.

It is clear that $J(\theta')$ in Eq. (1) is dependent, rigorously viewed, on both the kind of particle detected (i.e., electrons, protons, photons) and on the particle energy. However, in Section 2 it was noted that Detector A probably observed electrons quite predominately and within a fairly narrow energy range; hence, $J(\theta')$ is considered for only electrons of constant energy.

The integral Eq. (1) was solved for $J(\theta')$ by numerical procedures for each observed count rate curve $C_{obs}(\theta)$ as follows (the procedure described is a simplified one which evolved in an empirical way from more sophisticated and elegant methods):[1]

(1) $J(\theta')$ was assumed to be representable analytically by the 4th degree polynomial in θ',

$$J(\theta') = \sum_{k=0}^{4} a_k \, \theta'^{\,k} \quad ; \tag{2}$$

[1]An analysis was evolved employing Legendre polynomial expansions for $C(\theta)$, $S(\alpha)$, and $J(\theta')$ yielding a unique and simple result in that the coefficients for the $J(\theta')$ polynomial are given by a factor times the ratio of the count rate $C(\theta)$ polynomial coefficients to the response $S(\alpha)$ polynomial coefficients. However, it has not been possible so far to prevent the occurrence of negative values in the computations for $J(\theta')$ so this attractive method had to be abandoned.

where a_o, a_1, a_2, a_3 a_4 are to be evaluated or related through boundary conditions as follows:

(a) $J(\theta')$ is continuous with continuous first derivative at $\theta = 0°$, and $J(\theta')$ has vanishing first derivative at $\theta' = 0°$;

(b) $J(\theta')$ goes to zero at some $\theta' = \theta'_m$ near the θ value for which the count rate $C(\theta)$ goes to zero (Fig. 2c) as determined by the nature of the radiation being detected or a near zero value of $S(\alpha)$ (by Fig. 2b $S(\alpha)$ goes to zero near $\alpha = \pm 25°$).

(c) $J(\theta')$ approaches zero continuously (vanishing first derivative) at $\theta' = \theta'_m$.

(2) The assumed conditions (1 above) yielded a 4th degree polynomial in θ' containing two undetermined constants only.

(3) The $J(\theta')$ of Eq. (2) was represented by a step function (of small step-width $\Delta\theta'$ and $J(\theta')$ constant, J_i, within each $\Delta\theta'$) yielding the integral Eq. (1) in the form:

$$C(\theta) = \sum_{i=1}^{n} J_i \int_0^{2\pi} \int_{\theta_i' - \frac{\Delta\theta_i'}{2}}^{\theta_i' + \frac{\Delta\theta_i'}{2}} S(\alpha) \cos\theta' \, d\theta' \, d\phi' \; ; \qquad (3)$$

where

$$S(\alpha) = \exp(-\gamma_1 \alpha^2 - \gamma_2 \alpha^4),$$

and γ_1, γ_2 are shape parameters obtained from the response function measurement.

(4) The integrals in Eq. (3),

$$S_{ij} = \int_0^{2\pi} \int_{\theta_i' - \frac{\Delta\theta_i'}{2}}^{\theta_i' + \frac{\Delta\theta_i'}{2}} S(\alpha) \cos\theta' \, d\theta' \, d\phi' \tag{4}$$

were evaluated numerically using 5-degree intervals for both θ' and θ , and the indices i and j represent step values of θ' and θ , respectively.

(5) The a_k's of Eq. (2) were determined by a least squares solution of Eq. (3) in the form:

$$C(\theta_j) = \sum_{i=i}^{n} S_{ij} \; J_i \; , \tag{5}$$

where J_i was represented by

$$J_i = \sum_{k=o}^{4} a_k \; \theta_i'^{\,k}$$

following Eq. (2). With the a_k's evaluated, $J(\theta')$ followed from (2) and was plotted as in Fig. 2c.

(6) The process is then "reversed" for checking purposes; the calculated J_i's and the S_{ij}'s of (5) are employed to calculate count rates which are then compared with those originally observed. These count-rates agree well within the known experimental errors.

4. PRESENTATION OF DATA

The analyses of Section 2 yield a directional particle flux density distribution curve $J(\theta')$ vs. θ' (Fig. 2c) for each small neighborhood of space for which the directional count rate was measured. The basis for the presentation of the data (Figs. 4 through 9) are three well-known invariant quantities for the motion of geomagnetically trapped charged particles, as follows:

(1) The magnetic moment of the charged particle in its helical motion about a magnetic flux density line is constant to the extent that its cyclotron period is negligible compared to its "bounce" period (the time between successive reflections at the same mirror point) and the geomagnetic flux density variations are negligible throughout a cyclotron orbit. This adiabatic invariant relates the pitch angle (between particle momentum vector and geomagnetic flux density, $90 - \theta'$, as shown by Fig. 2a) of the charged particle at a spatial location where the magnetic flux density is $B_{satellite}$ to the magnetic flux density B_M at the mirror point (corresponding to a 90-degree pitch angle),

$$B_M = B_{satellite} / \cos^2 \theta' \quad . \tag{6}$$

(2) The complex motion of a charged particle in the geomagnetic field (a longitudinal helical motion combined with transverse drift due to the gradient and curvature of the geomagnetic field) is governed by the dynamical principle

stating that the action integral along a geomagnetic line is a constant. That is,

$$\oint m v_{\parallel}\, dl = S, \text{ a constant;} \tag{7}$$

where m is the charged particle mass; $v_{\parallel}$ is its speed tangent to the magnetic flux density $\vec{B}$; and dl is an element of path along $\vec{B}$. The use of the first invariant, Eq. (6), yields (7) in the form:

$$I, \text{ a constant} = \frac{S}{p} = \oint \left(1 - \frac{B}{B_M}\right)^{\frac{1}{2}} dl; \tag{8}$$

where p is the scalar momentum of the trapped charged particle. It is seen that I, the longitudinal invariant, has the dimension of length and is usually expressed in kilometers.

(3) The charged particle directional flux density in a static magnetic field is constant if measured always in the direction of the trajectory of a particular particle. This third invariant quantity is a consequence of Louiville's theorem.

These three invariants express the basic fact that the spatial variation of the trapped charged particle flux density is described fundamentally by constants of the motion of the particles in their trajectories rather than by geographic coordinates of altitude, latitude and longitude. The dynamical invariants have been discussed by several authors including Fermi and Rossi [1933], Lemaitre and Vallarta [1933] and Swann [1933] and more recently also by Northrop and Teller [1960]

and E. C. Ray [1959].

5. CONCLUSION

The essential purpose of the present paper is to present the directional flux densities of geomagnetically trapped charged particles as derived from Explorer IV data records in terms of both geographic coordinates and the invariants of the trapped particle motion as has been done in several equivalent ways in the series of figures in Section 4. In addition, the following comments may be made.

The pitch angles (angle between particle velocity vector and B-vector) of the trapped particles varies between a cutoff value of approximately 35° - 40° and 90° as is observed in Fig. 2c.

Some indication of the time constancy of the trapped particle radiation (probably electrons of around 700 kev energy) in the inner belt is given by the data and analysis (Fig. 2c) of passes 453 and 479 which occurred in nearly the same region of space (Fig. 3) with a time difference of nearly 2 days. It is noted (1) the maxima of the observed count rates are nearly identical, (2) the background count rates (for θ values greater than about 55°) are nearly identical indicating time constancy of the penetrating radiation, (3) the width of half-maximum of the count rate curves increased about 22 percent from pass 453 to pass 479. This width change corresponds to an angular width change of about 14°. Since it is estimated that the counter axis orientation (θ, Fig. 2a) determination may be in error by $\pm$ 10°, it can be stated that the count rate vs. θ curves for the two passes are identical within experimental limits. Hence, the inner zone particle entrapment appears to be stable for the time period noted.

The results of the present analysis can be compared with the neutron albedo theory calculations of Lenchek, Singer, et al [1961]. If the flux densities of Fig. 2c are for trapped electrons of about 700 kev in energy, as assumed in Section 2 above, the differential omnidirectional electron flux density obtained by estimating the area under the $J(\theta')$ curves of Fig. 2c is around $5 \times 10^2/cm^2$-sec-kev. The albedo theory value [Lenchek et al, 1961; Fig. 13] is about $4/cm^2$-sec-kev at 700 kev. Considering that the observed $500/cm^2$-sec-kev is for an uncertain energy interval above 700 kev, it appears that the observed particle flux density may be about an order of magnitude greater than theory predicts at 700 kev. It is interesting to note also that our observed differential omnidirectional electron flux density at 700 kev is about a factor of 2 larger than the observation of Walt, et al [1960] at somewhat lower electron energies.

ACKNOWLEDGMENTS

The authors wish to acknowledge the support of the Defense Atomic Support Agency (DASA) in this work. The cooperation of J. A. Van Allen and his colleagues and the calibration work of E. O. Baicy and his group were indispensable. We are indebted considerably also to Captain J. A. Welch, Jr. and his group at the Air Force Special Weapons Center, Kirtland Air Force Base, New Mexico, for the calculations of the integral invariant and the locations of the geomagnetic field lines. We acknowledge the help and interest of many of our colleagues at Marshall Space Slight Center, especially S. A. Fields, J. Kassner, F. Rodrigue, and R. D. Shelton.

TABLE I

SUMMARY OF RECENT INVESTIGATION OF CHARGED PARTICLES

IN THE EARTH'S MAGNETIC FIELD

(as of March 1, 1962)

A. PROTONS

Proton Energy, Location, etc.	Flux-Energy Spectrum References	Theoretical (mechanism for proton flux-energy calculation, or others)	Experimental	Lifetime of Trapped Protons τ_p ; other time constant
1. Energetic ($10-10^3$ Mev) component of Inner Van Allen Belt (Fig. 1)	1. Hess (1959): $\phi_p \propto E_p^{-1.30}$ protons/Mev cm^2-sec; E_p, energy in Mev	neutron albedo source plus loss by ionization only	deficiency of high energy (>200 Mev) protons	$\tau_p = 2.1 \times 10^{-9}\ MT^{1.24}$ sec, ($\tau_p \sim 10^9$ sec for 100 Mev at 100 km altitude)
	2. Singer (1959): Lenchek & Singer (1960)	neutron albedo source plus proton loss by ionization and breakdown of invariance of magnetic moment of higher energy protons	Hess (1959) states Singer-Lenchek theory disagrees with his measured spectrum	
	3. Alfvén (1959): $\phi_p \propto p^{-2.6}$, p is momentum	cosmic-ray spectrum modified by charged particle injection at a point with "magnetic pumping"	data of Freden and White (1960) in agreement	
	4. Freden and White (1960): $\phi_p = 1.55 \times 10^2 E_p^{-0.72}$, $E_p < 80$ Mev; $= 4.55 \times 10^{-17} f(E_p) \exp(-E_p/170)$, $E_p > 80$ Mev; (p, protons/Mev-cm^2-sec; in range 10-700 Mev; altitude, 1100 km)	neutron albedo source plus proton loss by ionization and nuclear collision loss (latter important for $E_p > 80$ Mev)	(1) good agreement with their own data in range 60-700 Mev (2) solar protons have little or no effect in range of observation; also, no other sun-source particles (alphas, etc.) were observed	$\tau_p = 3.5 \times 10^5 E_p^{1.31}$ sec (τ_p vs E_p plotted, Fig. 3)
	5. Armstrong, et al (1961): $\phi_p \propto E_p^{-1.8}$ protons/Mev-cm^2-sec in observation range 42 - 570 Mev		(1) qualitative agreement with F-W (1960) (2) total flux about 1/3 of F-W (1960) possibly due to altitude effect (3) above 100 Mev, data consistent with neutron albedo theory (4) below 100 Mev, some evidence for solar protons	
	6. Holly and Allen (1961): $\phi_p \propto E_p^{-n}$; n = 1.2 - 2.7, = 1.3 - 2.1 for different points in space		proton flux-energy curve plotted for 15° N latitude, 980 km altitude (Fig. 4)	
	7. Naugle and Kniffen (1961): directional and omnidirectional proton flux measured at different altitudes and latitudes but essentially same longitude. For 1600 km altitude, 21.5°N Lat. 235.4°W long, B = 0.209 gauss: $J(E_p) = 10^3 E_p^{-1.7}$; protons/Mev-cm^2-sec-sr ($40 \leq E_p \leq 100$ Mev), $4\pi J(E_p \geq 31) \sim 2400$ p/cm^2-sec	steepness of observed spectrum may be due to (1) failure of adiabatic invariance of proton magnetic moment (Singer), or to (2) solar protons trapped in geomagnetic field or to protons produced by albedo neutrons resulting from nuclear reactions of solar protons in the atmosphere over the polar caps	(1) proton spectrum (below 40 Mev) is much steeper than cosmic-ray spectrum (2) both shape of spectrum and proton flux change with latitude at same altitude and longitude	
	8. Hoffman, Arnoldy & Winckler (1962): at the maximum inner belt intensity (±29.2° mag. lat., 8660 km geocentric range) $\phi_p = 1.14 \times 10^4 E_p^{-1.66}$ protons/Mev-cm^2-sec, $E_p > 30$ Mev		(1) proton radiation softens with increasing geocentric range and latitude (2) data is not in disagreement with with other observations (Naugle & Kniffen, 1961; F-W, 1960; Armstrong, et al, 1961) or with neutron albedo mechanism	
	9. Freden and White (1962)		measured proton flux and energy spectrum (1000-1185 km altitude) (1) is in good agreement with previous measurements (1000-1230 km altitude), (2) agrees well with previous (neutron albedo) theory for 30-300 Mev, (3) above 300 Mev observed fluxes are less than theory due to loss mechanisms and inexact theory	
2. Outer Van Allen Belt	1. Inoue (1960)	protons are low energy (compared to electrons) due to large energy transfer for high energy protons to electrons, small energy transfer for high energy electrons to protons		
	2. Welch, et al (1959) Dragt, et al (1961)	hydromagnetic waves of resonant frequency affect proton magnetic moment if E_p is greater than energy corresponding to the resonance condition: $\lambda_{hm} = 2\pi R_{Cyclotron}$	(1) outer edge of Inner VA belt proton flux as function of position agrees well with neutron albedo theory (2) accounts for absence of protons in Outer VA belt (3) confirms original suggestion of Welch et al (1959)	for waves of about 1 gamma amplitude; 1 cps frequency; B, 0.04 gauss; E_p, 100 Mev; altitude, 2 R_E: proton lifetime is about 1 day
	3. Wentworth & Singer (1959)	low energy (about 20 kev) solar protons are lost by charge exchange with neutral hydrogen, as far out as 10 earth radii		
	4. D. G. Wentzel (1962)	hydromagnetic waves above proton belt systematically raise mirror points of proton orbits above the belt, especially if mirror points are near the atmosphere		lifetime of protons above proton belt is larger than a fraction of a day

B. ELECTRONS

Electron Energy, Location, etc.	Flux-Energy Spectrum References	Theoretical (mechanism for electron flux-energy calculation, or others)	Experimental	Lifetime of Trapped Electrons; Electrons; Other Time Constant
1. Component of both belts	1. Dessler & Karplus (1960): $\phi_e \alpha E_e^{-5}$ electrons/cm^2-sec	slow neutron albedo source with energy degradation due to electron-electron collisions (W. N. Hess & J. Poirer) for both belts	(1) considers Explorer IV and V data inconsistent with solar source of electrons in either belt because of minimum near 12.8 x 10^3 km above earth's surface (see (2) below) (2) considers Capetown anomaly as cause of electron belt minimum-anomaly lowers mirror altitude of trapped particles by about 10^3 km so emphasizing atmospheric absorption	about 1 year at high altitudes
	2. Inoue (1960)	Outer VA belt is a plasma: electron temperature, 2.4 x 10^8 °K (32 kev); electron density, 3.5 x 10^2/cm^3		
	3. Herlofson (1960)	injection of charged particles at 43 x 10^3 km (outside outer belt) + diffusion + acceleration by small magnetic field fluctuations	using diffusion coefficient αr^8, short diffusion time for second maximum of outer belt and long (100 times longer) diffusion time for the first maximum of outer belt yields agreement with experiment	
2. Inner VA Belt	4. Walt (1960)	electron spectrum at 1045 km not inconsistent with 750 kev cutoff (neutron albedo) but is softer and has high energy tail (Holly and Allen, 1961)	inner VA belt (1045 km, Wallops Island): electron flux (above 1 mev) + proton flux (above 1 mev) is less than 0.01 of electron flux 0.03-1 Mev	
	5. Holly and Allen (1961)	degraded neutron albedo spectrum (altitude, 980-1100 km; latitude, 15°N); in range 0-460 kev, softer than neutron β^--decay spectrum (perhaps hm wave loss, Parker, 1961)	(1) detector A counts (90% or more) electrons; detectors C, D count protons (2) bremsstrahlung correction, less than 5% (3) count rate intensity analysis is carried out	
	6. Lenchek, Singer & Wentworth (1961)	calculate trapped electron flux density from neutron albedo source and loss by small-angle coulomb scattering only at 1100 km on magnetic line extending to 1.5 earth radii	conclude, by comparison of theory and observations (Walt, et al, 1960; Cladis, et al 1961; Holly, 1960) albedo source is quantitatively valid for electron energies >400 kev	
	7. Hoffman, Arnoldy & Winckler (1962): at the maximum inner belt intensity (-28.4° mag. lat.) $\phi_e \sim 2. \times 10^9$ electrons/cm^2-sec $200 \leq E_e \leq 500$ kev; $\sim 10^7$ electrons/cm^2-sec $E_e > 500$ kev			
3. Outer VA Belt	8. Vernov, Chudakov, Vakulov, & Logachev (1959): $\phi_e \alpha E_e^{-6}$, $E_e > 50$ kev (ϕ_e, electrons/kev-cm^2-sec-sr)			
	9. Van Allen (1959) Arnoldy, Hoffman, & Winckler (1960), Helliwell & Bell (1960)	electrons accelerated to observed energies in geomagnetic field		
	10. Parker (1961)	outer VA belt electron loss by hm waves passing through a mirror point causing diffusion of charged particles; localized hm disturbances can result in limited particle acceleration but disturbances throughout geomagnetic field cause a net particle energy loss		hm wave of 10^{-4} gauss amplitude, 1 cps, causes 10^{-5}-ev electrons to diffuse along magnetic lines with a characteristic lifetime of 4 months
	11. Hess, Canfield, & Ligenfelder (1961)	neutron beta-decay source of belt electrons requires low-altitude electron ejection		
	12. Cladis & Dessler (1961)	solar injection of outer VA belt electrons no longer tenable considers origin of electrons (a) albedo neutron decay, and (b) local acceleration in geomagnetic field; suggests measurement of x-ray production near Capetown anomaly to evaluate (a)		time constant for renewal of electrons following magnetic dumping: (1) one day for local acceleration mechanism; (2) 10^{-9}-10^{10} sec for neutron decay source
	13. Rosen & Farley (1961)	irreversible mechanism for modulation of radiation count rates is required, in part	reversible betatron acceleration cannot account for all of Explorer VI observations	
	14. Dessler & Karplus (1961)	reversible, magnetic-storm-induced changes quantitatively account for some count rate variations		
	15. Cladis, Chase, Imhof, & Knecht (1961): $\phi_e \alpha 1.6 \exp(-0.022 E_e)$ electrons/kev-cm^2-sec-sr	neutron beta-decay plus other processes are required to explain Explorer VI electron flux distributions along a geomagnetic line of force	Flux-energy spectrum is best fit to Javelin sounding rocket data-has slope of E_e^{-6} only near E_e=350 kev	
	16. Hess, Killeen, et al (1961)	(1) spatial distribution of beta-decay electrons only is calculated with loss mechanisms (a) multiple small-angle Coulomb scattering (proportional to E_e^{-1}, approximately) resulting in velocity of lowering-mirror points (Welch, et al, 1959; Christofilos, 1959), important below 2000 km, and (b) slowing down by near collisions with thermal electrons (proportional to $E_e^{-0.8}$, approximately), important above 2000 km (2) calculated flux along a magnetic line (within 30° of the equator) is about 6 x 10^6 electrons/cm^2-sec	neutron beta-decay electrons (1) contribute significantly for energies >50 kev, and (2) more electrons are observed (Fan, et al, 1961) at low latitudes than predicted	
4. ARGUS electrons in slot	17. Welch & Whitaker (1959) Christofilos (1959)			for ARGUS 1 mev electrons, Table 1, p. 917; example: 10.2 days at 1200 km altitude

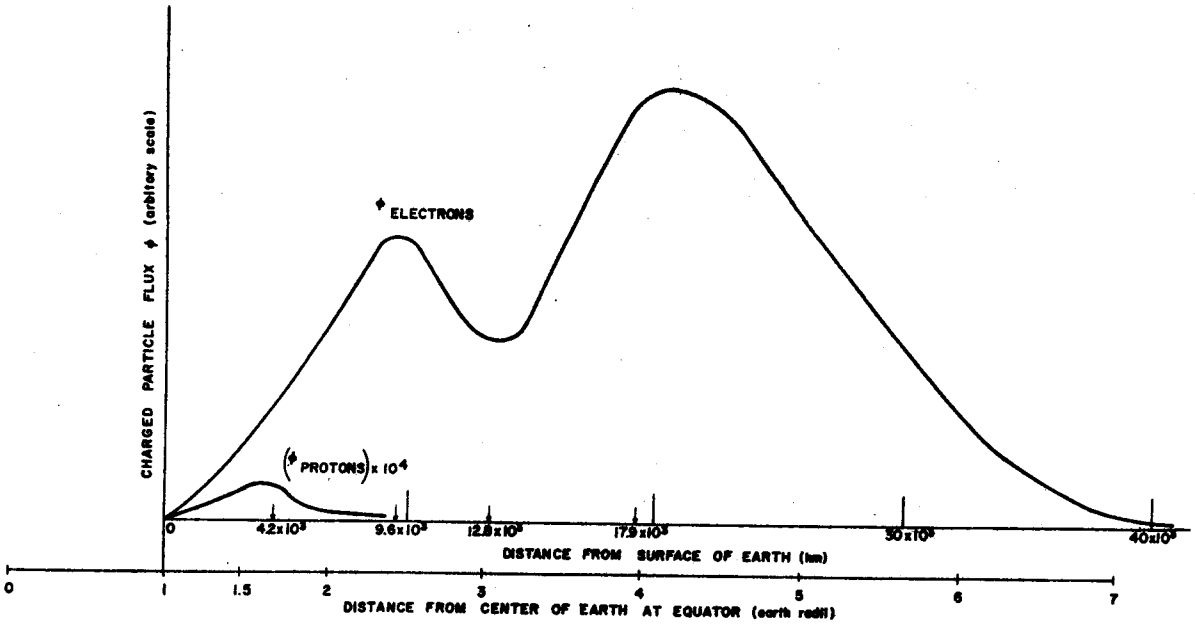

Fig. 1 Sketch showing essential topography in equatorial plane of the energetic flux (number/cm^2-sec) components of the charged particles (electrons and protons) trapped in the geomagnetic field.

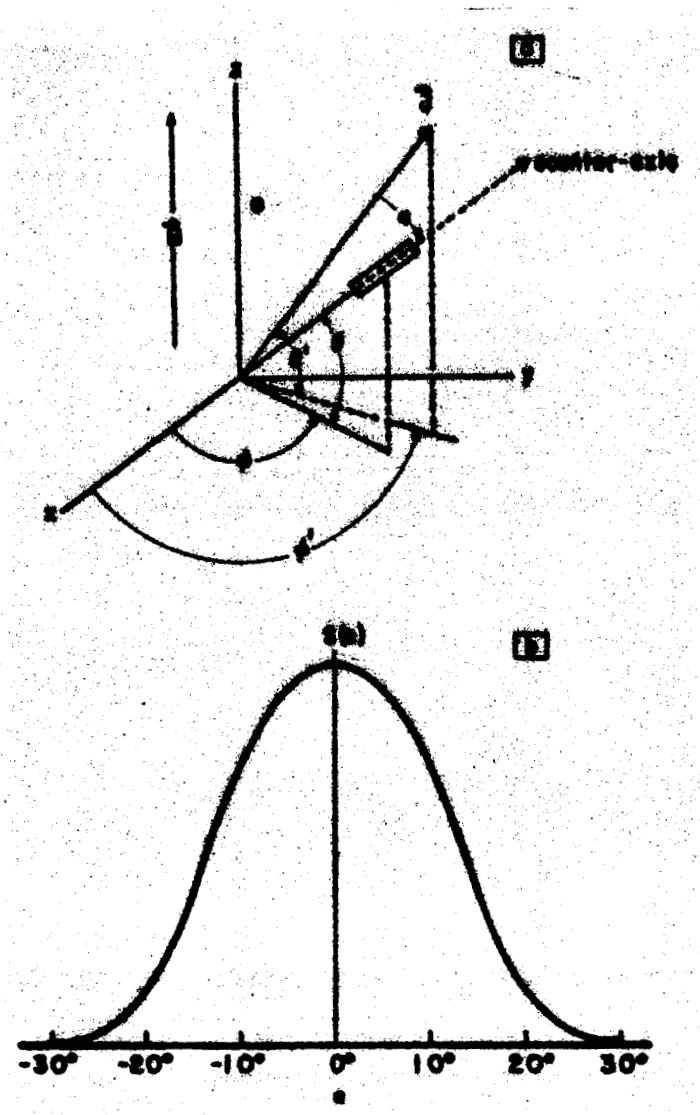

Fig. 2 (a & b) **Essential elements for directional analysis of satellite 1958 Epsilon (Explorer IV) Detector A count rates: a) the geometry relating the counter axis, geomagnetic field and directional particle flux density J , b) the counter response as a function of angle α as determined by E. O. Baicy.**

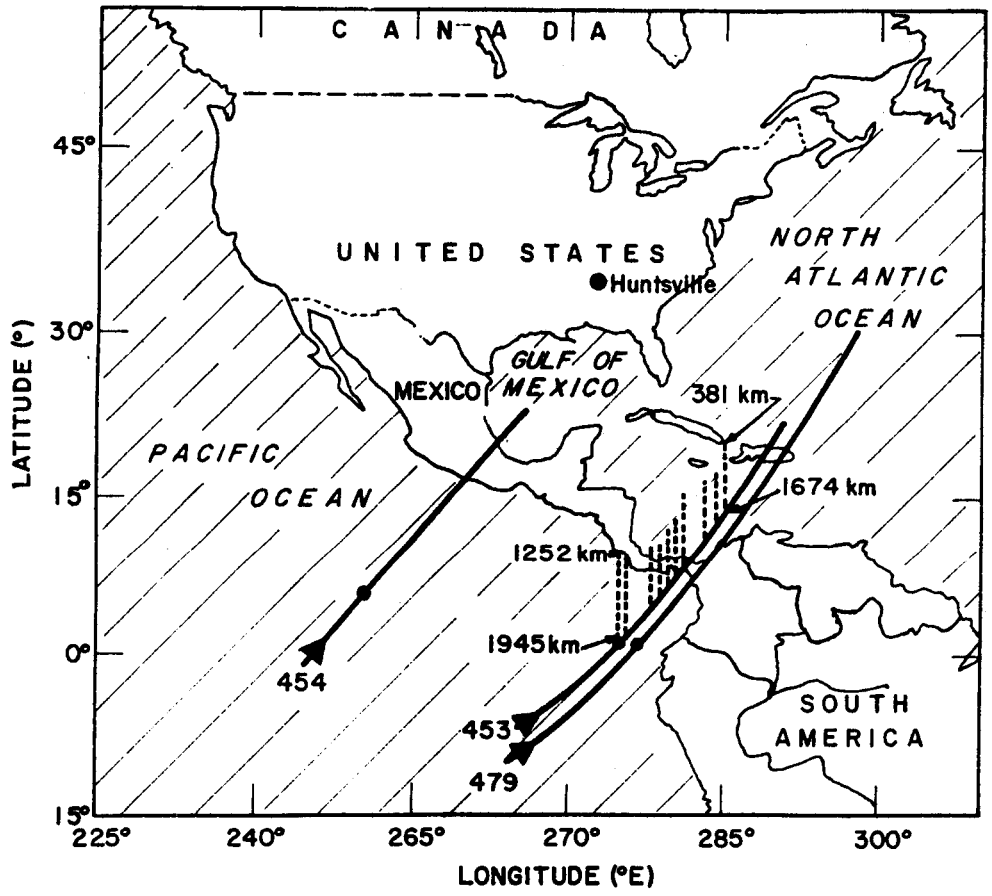

Fig. 3 Map showing location of satellite 1958 Epsilon (Explorer IV) for passes 453, 454, and 479 tracked by the U. S. Army Tracking Station at Huntsville, Ala. These passes were among those suitable for the analysis of the present investigation. Altitudes in km are indicated at several points. The vertical dashed lines beginning upon the trajectory for pass 453 are traces upon the earth's surface of geomagnetic field lines, passing through the satellite trajectory to lower altitudes, along which trapped particle mirror points are located as discussed in the text.

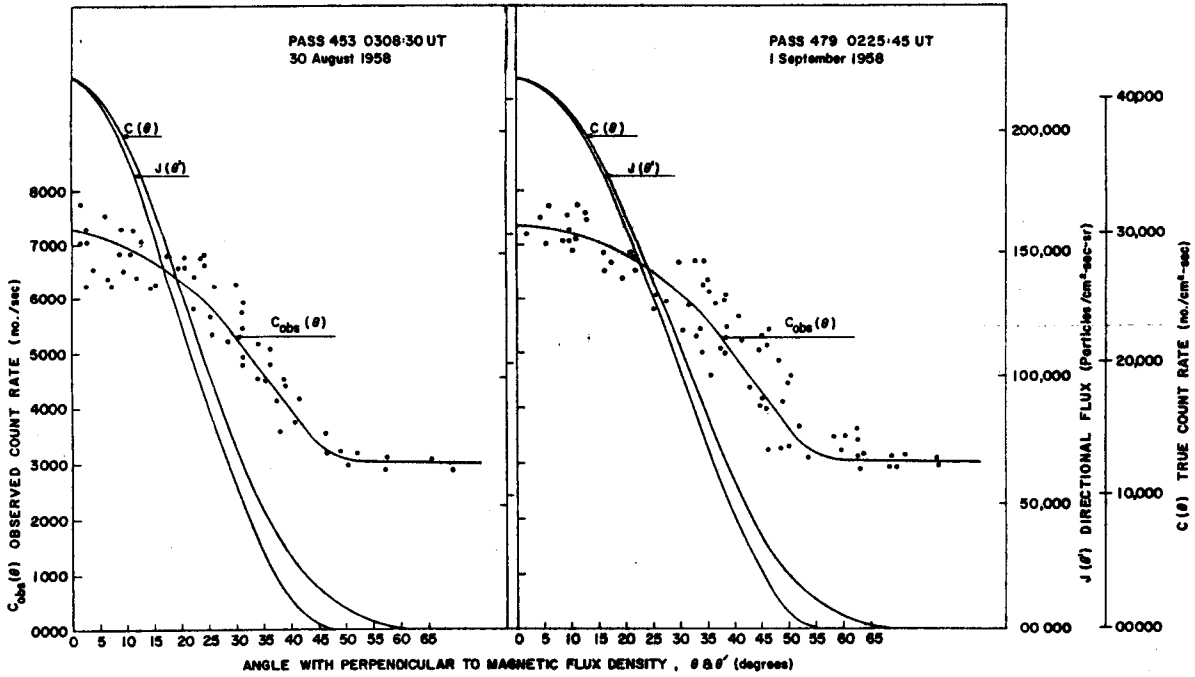

Fig. 2c The observed $C_{obs}(\theta)$, the corrected true $C(\theta)$ counts/cm²-sec, and the resultant directional intensity $J(\theta')$ no/cm-sec-sr as determined by the method described in Sect. 3. The two sets of curves represent observations at approximately the same point in the geomagnetic field but separated by about two days in time.

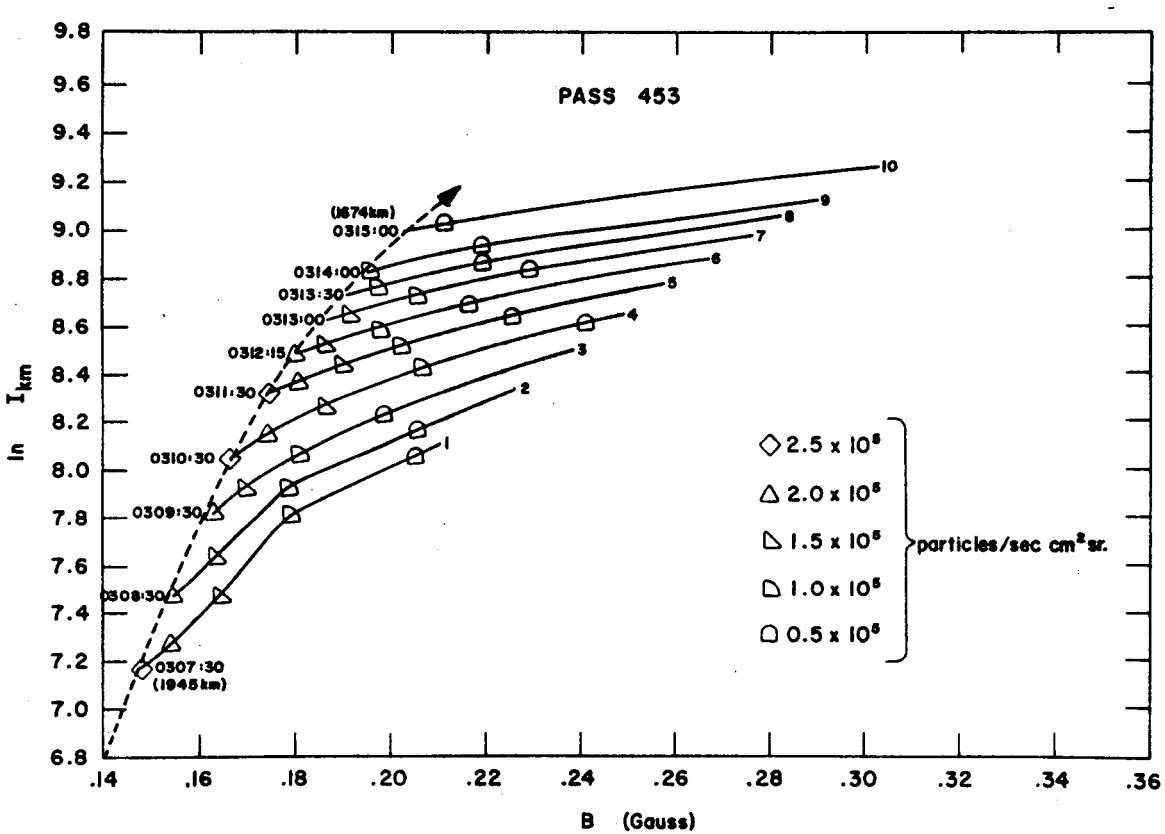

Fig. 4 The mirror point particle flux density distributions along B lines presented in terms of the dynamical invariants I in kilometers, (the second or longitudinal invariant defined by Eq. (8) and B. The data are from pass 453 (location shown by Fig. 3). The satellite trajectory is shown by dashes. The curves numbered 1 to 10 through the plotted points are B lines (shown also by Fig. 3) and the plotted points are directional particle flux densities $J(\theta)$ due to charged particles mirroring along a B line at the positions of the plotted points. Each set of B line points is derived from the directional count-rate of Detector A at the satellite position on the dashed trajectory.

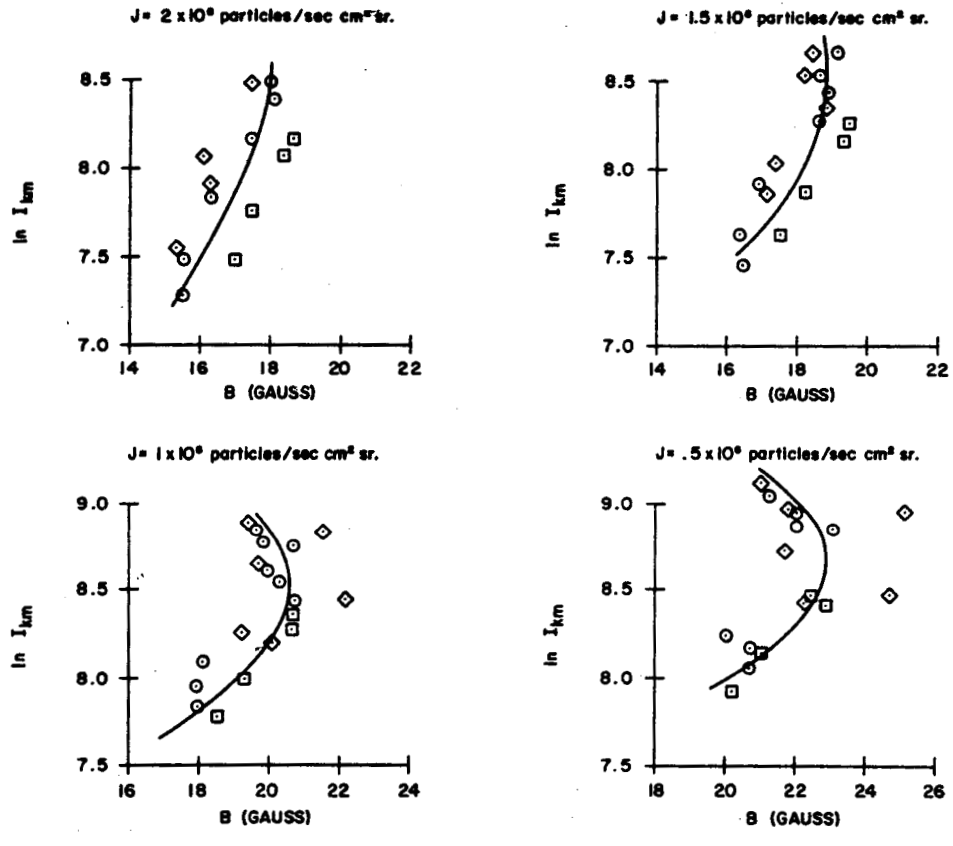

Fig. 5 The data of Fig. 4 plus similar data from passes 454 and 479, presented in terms of iso-J (particles/cm^2-sec-sr) plots. The solid lines are plotted from the least-squares reduction of the data points. The symbols for the plotted points represent the three passes: circles, pass 453; regular squares, pass 454; rotated squares, 479.

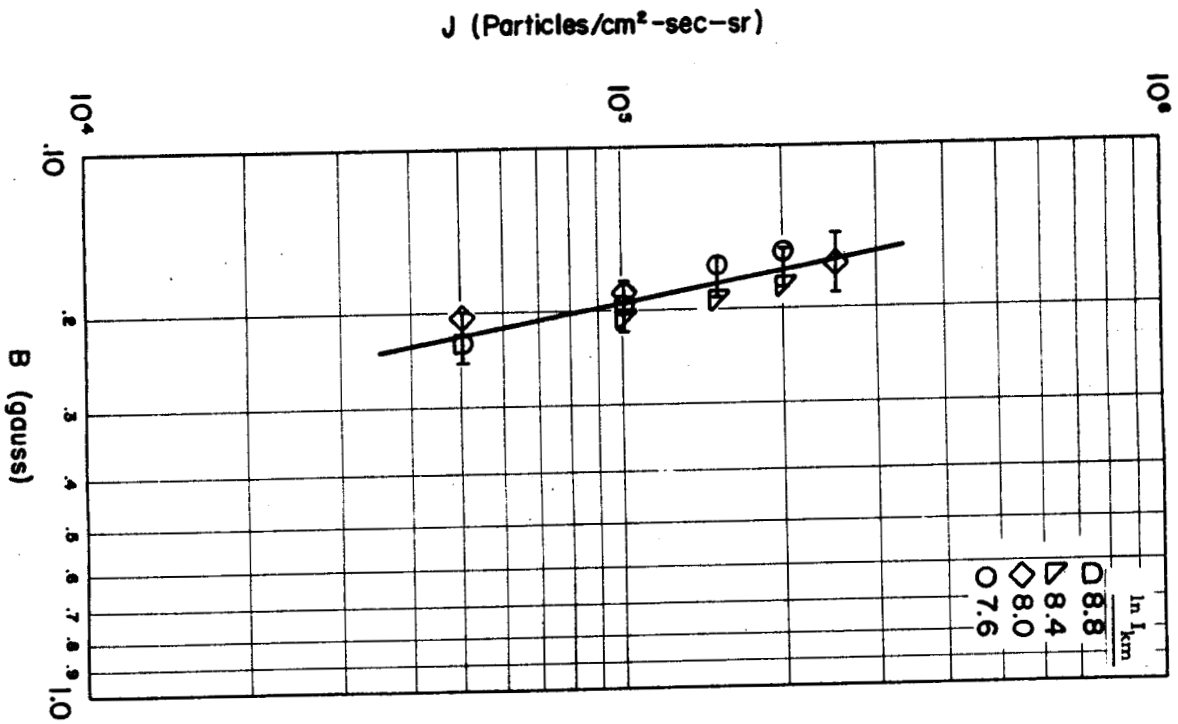

Fig. 6 The mirror point particle flux density distributions plotted vs. B at the mirror points. The data is the same as Fig. 5 and is plotted here in simplest form (using log scales). All plotted points are from pass 453 data; the horizontal bars indicated the maximum spread in B for all iso-J values for the data of all three passes 453, 454, and 479 (no points are shown for the latter two passes to avoid confusion). The equation of the straight line shown is $J = (\text{constant})\ B^{-n}$, where $n = 5.6$.

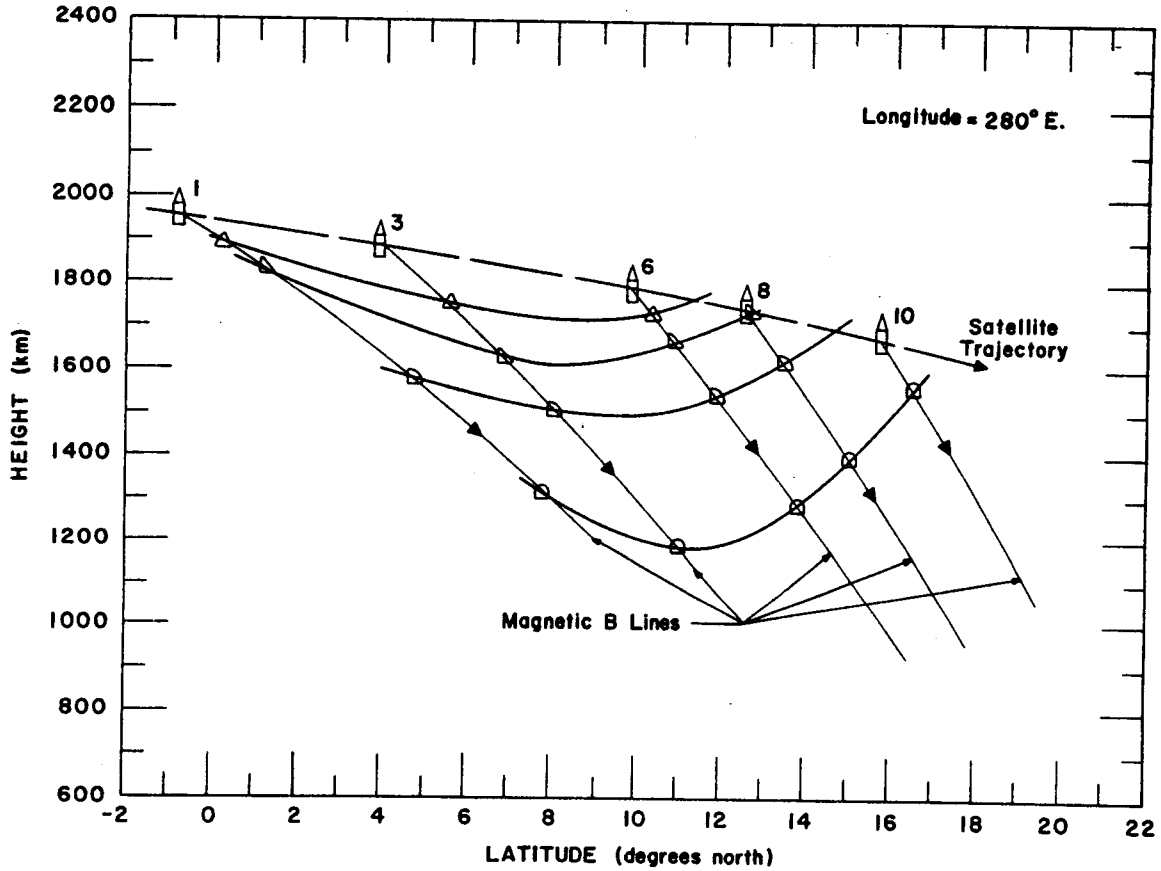

Fig. 7 A meridian plane projection (280°E longitude) showing the iso-J lines determined from this analysis. The bullet symbol indicates the satellite position at various times during pass 453. The B lines indicated by 1, 3, 6, 8, and 10, and the symbols used for the plotted points have the same meanings as in Fig. 4.

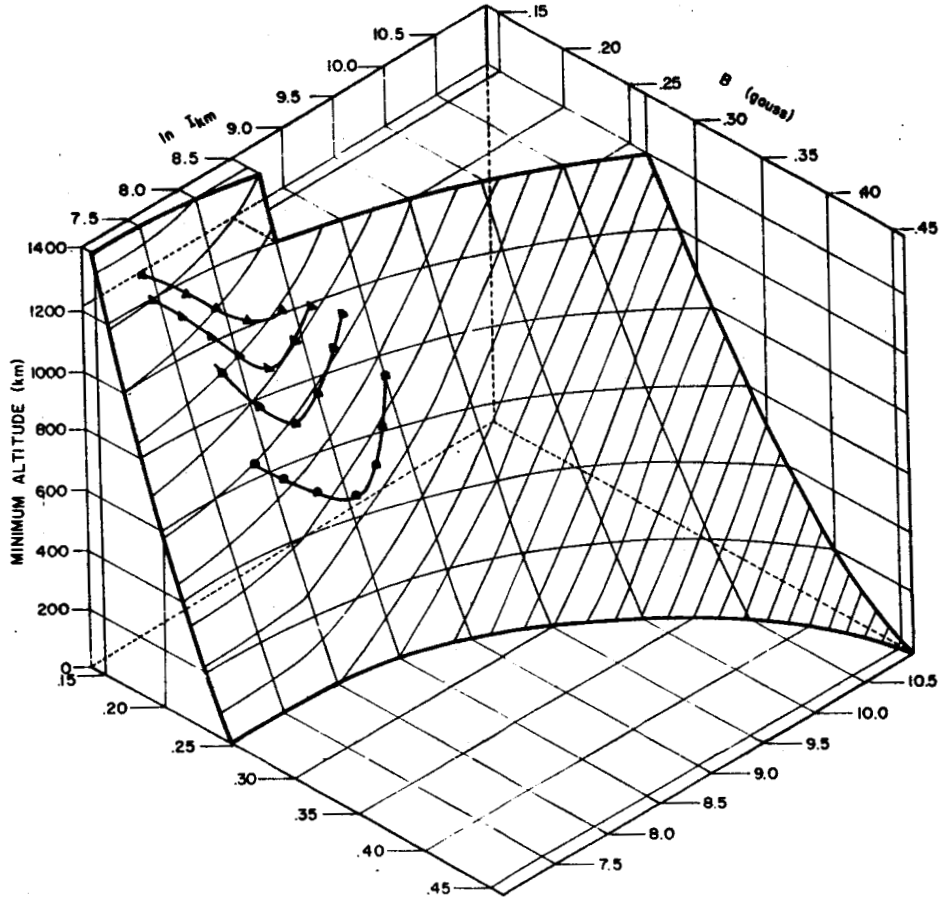

Fig. 9 Three-dimensional construction illustrating the relationship among the more significant parameters used in the present analysis: I, B and minimum altitude (lowest mirror altitude of a trapped particle during its total motion in the geomagnetic field). The curves shown are drawn from the data of Fig. 5. The symbols used for the plotted points have the same meaning as in Figs. 4 and 7.

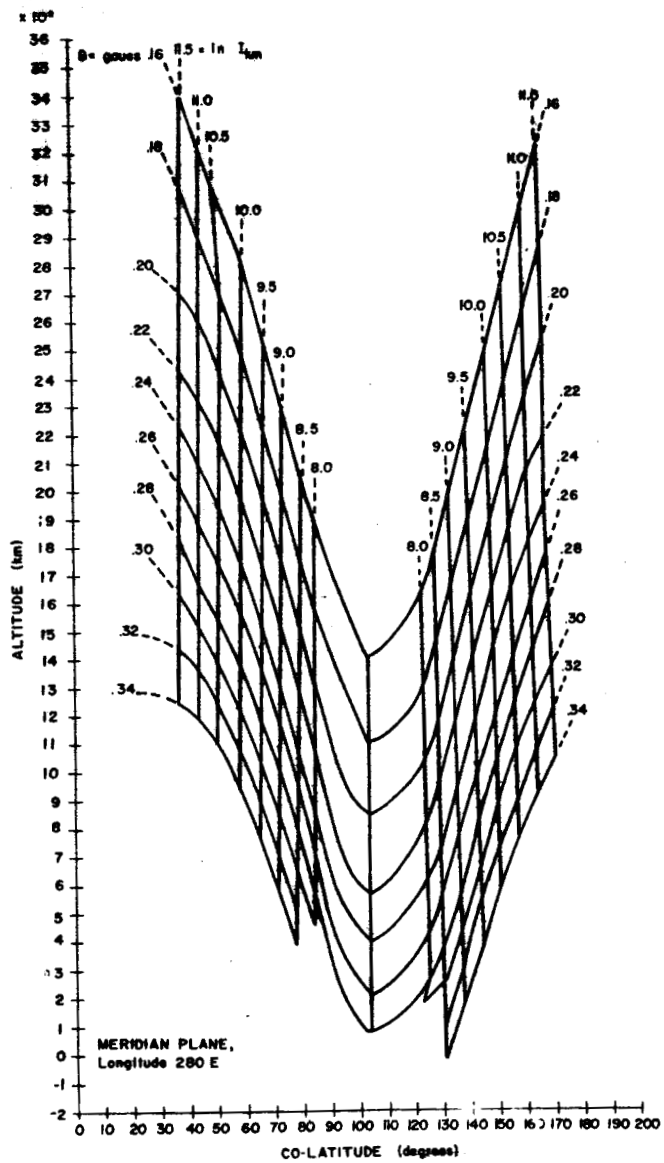

Fig. 8 Iso-I, iso-B grid constructed upon an altitude vs colatitude (90°- latitude in degrees) plot. This construction is convenient for relating the dynamical invariants I and B with the geographic coordinates of altitude, latitude, and longitude (constant). The plot is for the region of space around the pass 453 trajectory.

REFERENCES

Adams, R. M., Explorer IV - 1958 Epsilon Orbital Data Series, Issue 6, Smithsonian Astrophysical Observatory, Cambridge, Mass. and Army Ballistic Missile Agency, Redstone Arsenal, Ala., Nov. 1959.

Alfvén, H., Momentum spectrum of the Van Allen radiation, Phys. Rev. Ltrs. 3, 459, 1959.

Armstrong, A. H., F. B. Harrison, et al., Charged particles in the inner Van Allen radiation belt, J. Geophys. Res. 66, 351, 1961.

Arnoldy, R. L., R. A. Hoffman, et al., Observations of the Van Allen radiation regions during August and September 1959, Part I, J. Geophys. Res. 65, 1361, 1960; Solar cosmic rays and soft radiation observed at 5,000,000 kilometers from earth, J. Geophys. Res. 65, 3004, 1960.

Baicy, E. O., J. Boch, et al., Argus calibration of Explorer IV, 1958 epsilon, prototype, Ballistic Res. Labs, Aberdeen Proving Ground, March 1962.

Cladis, J. B. and A. J. Dessler, X-rays from Van Allen belt electrons, J. Geophys. Res. 66, 343, 1961.

Cladis, J. B., L. F. Chase, Jr., et al., Energy spectrum and angular distributions of electrons trapped in the geomagnetic field, J. Geophys. Res. 66, 2297, 1961.

Christofilos, N. C., The argus experiment, J. Geophys. Res. 64, 869, 1959.

Dessler, A. J. and R. Karplus, Some properties of the Van Allen radiation, Phys. Rev. Ltrs. 4, 271, 1960.

Dessler, A. J. and R. Karplus, Some effects of diamagnetic ring currents on Van Allen radiation, J. Geophys. Res. 66, 2289, 1961.

Dragt, A. J., Effect of hydromagnetic waves on the lifetime of Van Allen radiation protons, J. Geophys. Res. 66, 1641, 1961.

Fan, C. Y., P. Meyer, et al., The equatorial pitch-angle distributions of electrons in the outer radiation belt, Space Research, Vol. II (edited by Jager, Moore, and Van de Holst)N. Holland Pub. Co., 1962.

Fermi, E., and B. Rossi, Action of the earth's magnetic field on penetrating radiation, Accad. Lincei, Atti. 17, 346-350, 1933.

Freden, S. C. and R. S. White, Particle fluxes in the inner radiation belt, J. Geophys. Res. 65, 1377, 1960.

Freden, S. C. and R. S. White, Trapped proton and cosmic-ray albedo neutron fluxes, J. Geophys. Res. 67, 25, 1962.

Helliwell, R. A. and R. F. Bell, A new mechanism for accelerating electrons in the outer ionosphere, J. Geophys. Res. 65, 1839, 1960.

Herlofson, N., Diffusion of particles in the earth's radiation belts, Phys. Rev. Ltrs. 6, 414, 1960.

Hess, W. N., Van Allen belt protons from cosmic ray neutron leakage, Phys. Rev. Ltrs. 3, 11, 1959.

Hess. W. N., E. H. Canfield, et al., Cosmic-ray neutron demography J. Geophys. Res. 66, 665, 1961.

Hess, W. N., J. Killeen, et al., The observed outer-belt electron distribution and the neutron decay hypothesis, J. Geophys. Res. 66, 2313, 1961.

Hess, W. N. and J. Kileen, Spatial distribution of electrons from neutron decay in the outer radiation belt, J. Geophys. Res. 66, 3671, 1961.

Hoffman, R. A., Observations of the Van Allen radiation regions during August and September 1959. Part 2. The Capetown anomaly and the shape of the outer belt, J. Geophys. Res. 66, 4003, 1961.

Hoffman, R. A., R. L. Arnoldy, et al., Observations of the Van Allen radiations during August and September 1959. Part 3. The inner belt, J. Geophys. Res. 67, 1, 1962.

Holly, F. E., Radiation measurements to 1500 kilometers with Atlas pods, AFSWC Report TR-60-9, 1960.

Holly, F. E., L. Allen, Jr., et al., Radiation measurements to 1500 kilometer altitude of equatorial latitudes, J. Geophys. Res. 66, 1627, 1961.

Inoue, Y., Physical properties in the outer Van Allen belt and their relation to the phenomena in the exosphere, Space Research, Proc. First International Space Science Symposium (edited by H. Kallmann Bijl) N. Holland Publishing Co., 1960.

Jensen, D. C., R. W. Murray, et al., Tables of adiabatic invariants for the geomagnetic field 1955.0, AFSWC-TN-60-8, Kirtland AFB, April 1960.

Kellogg, P. J., Electrons of the Van Allen radiation, J. Geophys. Res. 65, 2705, 1960.

Lemaitre, G. and S. Vallarta, On Compton's latitude effect of cosmic radiation, Phys. Rev. 43, 87, 1933.

Lenchek, A. M. and S. F. Singer, Energy spectrum of geomagnetically trapped protons, Bull. Amer. Phys. Soc. 5, 47, 1960.

Lenchek, A. M., S. F. Singer, et al., Geomagnetically trapped electrons from cosmic ray albedo neutrons, J. Geophys. Res. 66, 2297, 1961.

Lundquist, C. A., R. J. Naumann, et al., Recovery of further data from 1958 epsilon, Space Research, Vol. II (edited by Jager, Moore, and Van de Holst) North Holland Pub. Co., 1962. Also IGY Satellite Report No. 14, Nat'l Acad. of Sci., Washington, D. C., July 1961.

Naugle, J. E. and D. A. Kniffen, Flux and energy spectra of the protons in the inner Van Allen belt, Phys. Rev. Ltrs. 7, 3, 1961.

Northrop, T. G. and E. Teller, Stability of the adiabatic motion of charged particles in the earth's field, Phys. Rev. 117, 215, 1960.

Parker, E. N., Effect of hydromagnetic waves in a dipole field on the longitudinal invariant, J. Geophys. Res. 66, 693, 1961.

Pletnev, B. D., The distribution of Corpuscular radiation in the stationary magnetic field of the earth, English Edition: Bull. Izuestiya, Acad. of Sci., USSR, Geophysics Series, No. 1, p. 95, January 1961.

Ray, E. C., On the application of Liouville's theorem to the intensity of radiation trapped in the geomagnetic field, State Univ. of Iowa, 1959.